JOURNAL OF PHYSICAL ORGANIC CHEMISTRY
J. Phys. Org. Chem. 2006; **19:** 43–52
Published online 30 August 2005 in Wiley InterScience (www.interscience.wiley.com). DOI: 10.1002/poc.987

Fluorescence and photoisomerization studies of *p*-nitrophenyl-substituted ethenylindoles

Anil K. Singh* and Prasanta K. Hota

Department of Chemistry, Indian Institute of Technology, Bombay, Powai, Mumbai 400 076, India

Received 24 January 2005; revised 20 June 2005; accepted 5 July 2005

ABSTRACT: The synthesis, electronic absorption, fluorescence (λ_f, λ_{ex}, Φ_f, τ_f) and photoisomerization ($\Phi_{t\rightarrow c}$, photostationary state composition) properties of 3-(4-nitrophenylethenyl-*E*)-NH-indole (**1**), 3-(4-nitrophenylethenyl-*E*)-*N*-ethylindole (**2**) and 3-(4-nitrophenyl ethenyl-*E*)-*N*-benzenesulfonylindole (**3**) in organic solvents of varying polarity are reported. The absorption maximum of these compounds undergoes a moderate red shift with increasing solvent polarity. However, the fluorescence maximum becomes highly red shifted with increasing solvent polarity. Whereas **1** and **2** show broad fluorescence bands, **3** exhibits dual fluorescence. Further, **1** and **2** fluoresce much more efficiently than **3**. Correlation of the Stokes shift with solvent polarity parameters such as Δ_f and $E_T(30)$ and excited-state dipole moment indicate a highly polar excited state for **1**–**3**. Time-resolved fluorescence studies show that the fluorescence decays are single- and multi-exponential type, depending on the solvent polarity. Further, **1** and **2** do not show photoisomerization on irradiation. However, **3** is photoactive and shows efficient photoisomerization in non-polar heptane. The sensitivity (ρ) of the photoreaction is determined in various solvent in terms of the Hammett plot, which showed that the excited states involved are electron deficient in nature and consequently stabilized more by an electron sufficient polar solvent and electron donating substituent. These results led us to suggest the existence of three types of excited states, namely the locally excited state, the intramolecular charge-transfer excited state and the conformationally relaxed intramolecular charge-transfer excited state in the photoprocesses of these compounds.

KEYWORDS: indole; ethene; fluorescence; photoisomerization; charge transfer

INTRODUCTION

The photochemistry and photophysics of 1,2-diphenylethene has been extensively examined and reviewed.[1–6] This is partly because 1,2-diphenylethene (stilbene) and its longer homologues (collectively known as α,ω-diphenylpolyenes) serve as a model for photobiologically significant linear polyenes such as retinal, carotenoids and their lower homologues.[7–12] Additionally, these compounds exhibit interesting electro-optical properties that can find applications in sensors, optical brighteners, laser dyes, optical data storage systems, photoconductors, photochemical cross-linking of polymers, non-linear optics, etc.[13–16] In this context, photoinduced intramolecular charge transfer in donor–acceptor conjugated polyenes such as stilbene and its derivatives have attracted a great deal of attention in recent years. It is found that the singlet excited state (S_1) of *trans*-stilbene is highly substituent and solvent polarity sensitive and is relatively stabilized in polar solvents. Upon excitation, the S_1 state of *trans*-stilbene competes with its activated twisting to a perpendicular (P*) species, which subsequently leads to its *cis–trans* photoisomerization. The double bond twisted perpendicular species (P*) is weakly polar and follows the non-radiative pathway to the ground state. On the other hand, when the excited state has more polar character, its rapid stabilization causes considerable energy gap between the P* and charge-transfer (CT) excited species, which leads to efficient fluorescence. Substituents can raise or lower the torsional energy barrier and thus the fluorescence quantum yields for substituted stilbene compounds are altered. In nitro-substituted stilbenes, butadienes and hexatrienes and in their stiffened derivatives, a highly polar excited-state species is believed to be formed upon excitation, which becomes stabilized more than the P* state even in relatively non-polar solvents[17–22] and such compounds follow the radiative pathway rather than the phantom excited state (P*) pathway. Recently, we reported large solvatochromic/dual fluorescence in nitro-substituted diarylbutadienes.[23–26] These systems in general, however, fluoresce very inefficiently.

It is widely accepted that in such push–pull molecules the solvent polarity-driven dual fluorescence can occur owing to the emission from an initially prepared planar locally excited state (LE) and from a CT state formed through subsequent conformational relaxation. Thus, various mechanisms have been proposed in order to explain the photo-induced charge separation in push–pull

**Correspondence to:* A. K. Singh, Department of Chemistry, Indian Institute of Technology, Bombay, Powai, Mumbai 400 076, India.
E-mail: retinal@chem.iitb.ac.in

systems, which include a twisted intramolecular charge-transfer (TICT) mechanism,[27,28] planarized intramolecular charge-transfer (PICT) state or pseudo-Jahn–Teller state[29,30] and rehybridized intramolecular charge-transfer state (RICT).[31,32]

While the excited states of nitrostilbenes and their *N*,*N*-dimethyl derivatives have been extensively studied, little attention has been paid to the *N*-substituted acceptor systems. To the best of our knowledge, the photophysical studies of ethenes bearing indole as one of the donor substituents are limited. Therefore, it was thought desirable to investigate such compounds to obtain more information regarding the nature of the CT excited states in donor–acceptor ethenes. In this context, we prepared *p*-nitrophenyl-substituted ethenylindoles, namely, 3-(4-nitrophenylethenyl-*E*)-NH-indole (**1**), 3-(4-nitrophenylethenyl-*E*)-*N*-ethylindole (**2**) and 3-(4-nitrophenylethenyl-*E*)-*N*-benzenesulfonyl indole (**3**) (Scheme 1) and examined the effect of *N*-substituted electron-acceptor and electron-donor substituents on the absorption, fluorescence and photoisomerization properties of these push–pull compounds. The nitroaryl group (σ_p: +0.81) can act as a strong acceptor and the indole moiety can act as an electron donor. Further, the donor ability can be altered by putting an electron-releasing ethyl group (σ_p: −0.14 for CH_3) or an electron-withdrawing group such as benzenesulfonyl (σ_p: +0.73 for SO_2CH_3) by replacing hydrogen at the nitrogen atom. Hence, these compounds represent novel push–pull ethenes, which have been examined for their excited-state properties.

EXPERIMENTAL

General methods

Indole-3-aldehyde and *p*-nitrophenyl acetic acid from Aldrich Chemical Co. USA, were used as received. All solvents were of AR or UV grade and further dried and distilled. The light petroleum used was of the b.p. 60–80 °C fraction. Melting-points were determined on a Veego melting-point apparatus. UV–visible measurements were made on Shimadzu UV-160A spectrophotometer. FTIR spectra in KBr discs were recorded on a Nicolet Impact 400 spectrophotometer. ^{1}H NMR spectra in $CDCl_3$ using TMS as internal standard were recorded on a Varian VXR 300 MHz FT-NMR instrument. CHN analyses were performed on a Theoquest CE 1112 Series CHNS autoanalyzer. HPLC analyses were performed on a Beckman instrument consisting of a Beckman Model 110A pump and a Model 340 organizer fitted with a wavelength-selective absorbance detector. The fluorescence spectra of **1**–**3** in all the solvents at 298 K were recorded on a DM1B microprocessor-controlled Spex-112 Fluorolog spectrofluorimeter equipped with Spex-1932 F accessories. The samples were excited at their absorption wavelength maximum (λ_{abs}). The fluorescence quantum yield (Φ_f) at 298 K was determined by taking Rhodamine B in ethanol as standard (Φ_f, 0.69),[33] and using the following equation: $\Phi = \Phi^{ref}(\eta^2_{ref}/\eta^2) \times (OD_{ref}/OD) \times (A/A_{ref})$, where η and η_{ref} are the refractive indices of the solvents, OD and OD^{ref} are the optical densities, Φ and Φ^{ref} are the fluorescence quantum yields and A and A^{ref} are the areas of the fluorescence bands of the compound and the reference standard, respectively. Time-resolved fluorescence decay measurements were carried out using a high repetition rate picosecond laser coupled to a time-correlated single photon counting (TCSPC) spectrometer (Hamamatsu 2809). Samples were excited in the absorption band of the compounds at 315 nm by vertically polarized picosecond laser pulses (frequency-doubled Ti:sapphire laser). The emission was collected at the peak in the 350–600 nm region. The typical peak count was 1000–5000. The quality of the exponential fits was evaluated by the reduced χ^2 value ($\sim$1.2). The excited-state dipole moments for all the

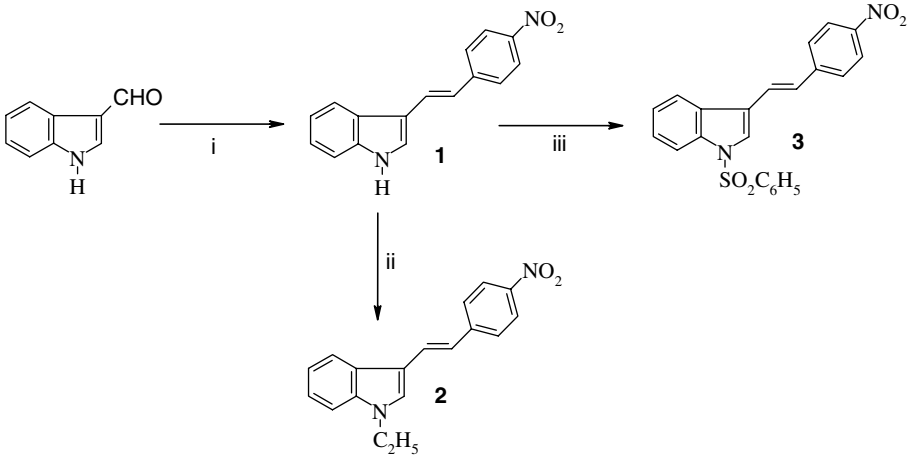

Scheme 1. Synthetic scheme for **1**–**3**. Reagents and reaction conditions: (i) *p*-nitrophenylacetic acid, pyridine–piperidine, reflux, 100 °C, 8 h; (ii) potassium-*tert*-butoxide, *tert*-butyl alcohol, ethyl bromide, reflux, 12 h; (iii) benzenesulfonyl chloride, acetone, K_2CO_3, r.t., 3 h

compounds were calculated using the ground-state dipole moments (determined by the semiempirical AM1 method,[34] geometry optimization, convergence limit = 0.000 000 1, iteration limit = 32 357) and the slopes obtained from the Lippert–Mataga equation:[35] $\nu_a - \nu_f = \{[2(\mu_e - \mu_g)^2/hca^3]F(\varepsilon,\eta)\}$, where $\nu_a - \nu_f$ is the Stokes' shift, μ_e and μ_g are the excited-state and ground-state dipole moments, respectively, $\mu_e - \mu_g = \Delta\mu$ is the change in dipole moment, h is Planck's constant, c is the velocity of light, a is the Onsager cavity radius and $F(\varepsilon,\eta) = \Delta f$ is the solvent polarity parameter. Further, $\Delta f = (\varepsilon - 1)/(2\varepsilon + 1) - (\eta^2 - 1)/(2\eta^2 + 1)$, where ε is the relative permittivity and η is the refractive index[36] of the solvent. For Onsager radius parameter a, we used a value of 7.3 Å, which is a reported value for a similar ethene (*N*,*N*-dimethylamino-*p*-nitrostilbene).[22] For all electronic spectroscopic studies, 2.0×10^{-5} M solutions were used.

For photoisomerization studies, 1.0×10^{-3} M solutions of **1**–**3** were irradiated at 365 nm using a 400 W medium-pressure mercury lamp (Applied Photophysics, London, UK) equipped with a monochromator. Irradiated solutions were analyzed using HPLC and ^{1}H NMR spectroscopy. The photoisomerization quantum yield ($\Phi_{t\rightarrow c}$) was determined using the potassium ferrioxalate actinometry method.[37] The amount of *trans* photoisomer that disappeared during irradiation was determined by HPLC analysis. The number of quanta absorbed was determined by irradiating 2 ml of the ferrioxalate solution (0.006 M) and assuming the quantum yield of formation of Fe^{2+} ion to be 1.21. Using the percentage disappearance of *trans* isomers, action plots were drawn.

Syntheses

3-(4-Nitrophenylethenyl-*E*)-NH-indole (1). 3-Formylindole (1.45 g, 0.01 mol) was taken in freshly distilled pyridine (10 ml) along with piperidine (0.6 ml) and *p*-nitrophenylacetic acid (1.81 g, 0.01 mol) in a round-bottomed flask fitted with a reflux condenser. The reaction mixture was heated at around 100 °C for 6 h. The progress of the reaction was monitored by TLC (15% ethyl acetate in light petroleum, $R_f = 0.2$). The reaction mixture was cooled to room temperature, poured into ice-cold water and treated with 100 ml of dilute hydrochloric acid to remove excess of pyridine from the reaction mixture. The brick red product was filtered and purified by column chromatography (silica gel, 10% ethyl acetate in light petroleum). Yield 19%; $R_f = 0.2$ [ethyl acetate–light petroleum (1.5:8.5)]; HPLC, retention time $t_R = 8.3$ min [LiChrosorb Si-60, 5 µm, 250 × 4 mm i.d., ethyl acetate–hexane (2:8), flow rate 2 ml min^{-1}, detector wavelength 405 nm); m.p. 142–144 °C; UV–visible (MeOH) λ_{max} (nm) (ε, 1 mol^{-1} cm^{-1}: 413 nm (20 000); FTIR ε(cm^{-1}): 3363 (NH), 1591,1342 (NO_2), 1637 (C═C); ^{1}H NMR: δ7.17 (d, $J = 16.4$ Hz, 1H, —CH═C—$ArNO_2$), 7.25–7.33 (m, 2H at C-5 and C-6), 7.41–7.45 (m, 1H, C-7), 7.47 (s, 1H, H—C_2), 7.51 (d, $J = 16.4$ Hz, 1H, —C═CH—$ArNO_2$), 7.61 (d, $J = 8.4$ Hz, 2H, —Ar), 7.99–8.02 (m, 1H, —H—C_4), 8.22 (d, $J = 8.7$ Hz, 2H, —$ArNO_2$), 8.34 (s, br, 1H, —NH). Elemental analysis. calcd for $C_{16}H_{12}N_2O_2$ (264.3): C, 72.71; H, 4.57; N,10.60. Found: C, 72.57; H, 4.54; N, 10.78%.

3-[4-Nitrophenylethenyl-*E*]-*N*-ethylindole (2). Compound **1** (0.5 g, 0.002 mol) was taken in freshly distilled *tert*-butyl alcohol (20 ml) and potassium *tert*-butoxide (0.2 g, 0.002 mol) in a two-necked round-bottomed flask fitted with a reflux condenser. The reaction mixture was stirred for 30 min at room temperature. Ethyl bromide (2 ml, 0.01 mol) was added to the reaction mixture and stirring was continued. A white suspension was formed. It was further refluxed at 100 °C for 12 h. The progress of the reaction was monitored by TLC (15% ethyl acetate in light petroleum, $R_f = 0.45$). The reaction mixture was cooled to room temperature, poured into ice-cold water and kept at 4 °C for 1 day. A yellow crystalline product was filtered. It was further purified by column chromatography (silica gel, 5% ethyl acetate in light petroleum). Yield 80%; $R_f = 0.45$ [ethyl acetate–light petroleum (1.5:8.5)]; HPLC, $t_R = 6.66$ min [LiChrosorb Si-60, 5 µm, 250 × 4 mm i.d., ethyl acetate–hexane (1.5:8.5), flow rate 1.1 ml min^{-1}, detector wavelength 405 nm]; m.p. 135–136 °C; UV–visible (MeOH) λ_{max} (nm) (ε, l mol^{-1} cm^{-1}): 418 (18 823); FTIR ν_{max} (cm^{-1}): 1596, 1331 (NO_2), 1627 (C═C); ^{1}H NMR: δ1.51(t, $J = 7.32$ Hz, 3H, CH_3), 4.21(q, $J = 7.32$ Hz, 2H, CH_2), 7.12 (d, $J = 16.1$ Hz, 1H, —CH═C—$ArNO_2$), 7.23–7.34 (m, 2H, C-5, C-6), 7.38 (s, 1H, C-7), 7.40 (s, 1H, C-2), 7.49 (d, $J = 16.4$ Hz, 1H, —C═CH—$ArNO_2$), 7.59 (d, $J = 8.7$ Hz, 2H, Ar), 7.98–8.00 (m, 1H, C-4), 8.20 (d, $J = 8.7$ Hz, 2H, —$ArNO_2$). Elemental analysis. Calcd for $C_{18}H_{16}N_2O_2$ (292.3): C, 73.99; H, 5.51; N, 9.58. Found: C, 73.99; H, 5.09; N, 9.51%.

3-[4-Nitrophenylethenyl-*E*]-*N*-benzenesulfonylindole (3). Compound **1** (0.1 g, 0.4 mmol) in acetone (10 ml) and anhydrous potassium carbonate (0.5 g, 4 mmol) were taken in a round-bottomed flask fitted with a reflux condenser. The reaction mixture was stirred at room temperature for 30 min, then cooled to 0 °C in a crushed-ice bath and benzenesulfonyl chloride (0.1 ml, 0.8 mmol) was added dropwise to the reaction mixture and stirring was continued. The progress of the reaction was monitored by TLC (silica gel, 15% ethyl acetate in light petroleum). The product was filtered and the organic solvent was evaporated under reduced pressure. The light-yellow compound was purified by column chromatography (silica gel, 5% ethyl acetate in light petroleum). Yield 85%; $R_f = 0.4$ [ethyl acetate–light petroleum (1.5:8.5)]; HPLC: $t_R = 13$ min [LiChrosorb Si-60, 5 µm, 250 × 4 mm i.d., ethyl acetate–hexane (1.0:9.0), flow rate, 1.1 ml min^{-1} at detector wavelength 365 nm]; m.p.: 177–178 °C; UV–visible (MeOH) λ_{max} (nm) (ε,

$1\,mol^{-1}\,cm^{-1}$): 367 (16 561); FTIR ν_{max} (cm^{-1}): 1597, 1334 (NO_2) 1640 (—C═C—), 1183(—S═O); ^1H NMR: δ7.22 (d, $J = 18$ Hz, 1H, —CH═C—$ArNO_2$), 7.29 (d, $J = 18$ Hz,1 H, —C═CH—$ArNO_2$), 7.34–7.43 (m, 2 H, H at C-5 and C-6), 7.44–7.56 (m, 3H, benzenesulfonyl proton), 7.62 (d, $J = 9$ Hz, 2 H, Ar), 7.81–7.87 (m, 2H, near sulfonyl, benzene proton), 7.92 (m, 2H, H—C-7 and H—C-2), 8.05 (m, 1H, H—C-4), 8.22 (d, $J = 9$ Hz, 2 H, $ArNO_2$). Elemental analysis. Calcd for $C_{22}H_{16}N_2O_4S$ (404): C, 65.33; H, 3.98; N, 6.92, S, 7.92. Found: C, 65.20; H, 3.88; N, 6.82; S 7.95%.

3-[4-Nitrophenylethenyl-*Z*]-*N*-benzenesulfonylindole (*cis*-3). A solution of *trans*-**3** [0.01 g in 10 ml of heptane–1,4-dioxane mixture (1:1, v/v)] was irradiated for 2 h with a medium-pressure mercury lamp using a glass filter with 350/400 nm cut-off (transmittance at 350 nm 50% and at 400 nm 100%). The reaction mixture was concentrated in vacuum and the *cis* product was isolated by conventional preparative TLC, which provided 3 mg of *cis*-**3**. Yield 50% (with respect to *trans*); TLC $R_f = 0.42$ [ethyl acetate–light petroleum (1.5:8.5)]; HPLC $t_R = 12$ min (13 min for *trans*) (LiChrosorb Si-60, 5 μm, 250 × 4 mm i.d., 10% ethyl acetate–hexane, flow rate, 1.1 ml min^{-1} at detector wavelength 365 nm); UV–visible (MeOH) λ_{max} (nm): 363; ^1H NMR: δ6.78 (1H, s, H at —In—C_2), 7.17 (1H, d, $J = 8$ Hz, —CH═C—$ArNO_2$), 7.19 (1H, d, $J = 8$ Hz, —C═C*H*—$ArNO_2$), 7.28–7.40 (2H, m, H at —In—C-4 and —C-7), 7.42–7.50 (3H, m, benzenesulfonyl proton), 7.52–7.68 (2H, m, near sulfonyl, benzene proton), 7.81 (2H, d, $J = 9$ Hz, Ar), 7.99 (2H, d, $J = 9$ Hz, $ArNO_2$), 8.17 (1H, d, H at —In—C-5), 8.23 (1H, d, H at —In—C-6).

RESULTS AND DISCUSSION

Absorption and fluorescence studies

Absorption and fluorescence spectral data for **1**–3 in organic solvents of different polarity are given in Table 1. Typical absorption spectra of **1** and **3** are shown in Fig. 1. A moderate red shift in the absorption maximum ($\lambda_{abs\ max}$) with increasing solvent polarity is observed for all the compounds. In protic polar solvents such as methanol, the $\lambda_{abs\ max}$ is comparable to that in the aprotic polar solvents. This indicates the absence of ground-state hydrogen bond interactions in these compounds. The moderate red shift in $\lambda_{abs\ max}$ can, therefore, be due to mesomeric effects and intramolecular charge transfer from the donor to the acceptor moiety. The ground-state dipole moment (**1**, 8.50 D; **2**, 8.91 D; **3**, 7.86 D) as determined by the Hyperchem semiempirical AM1 method indicates that in the ground state compounds **1**–**3** are polar in nature.

In contrast to a rather moderate solvent polarity effect on their $\lambda_{abs\ max}$, **1**–**3** show a marked influence of solvent polarity on their fluorescence maximum ($\lambda_{f\ max}$). Typical fluorescence emission and excitation spectra of **1** and **3** are shown in Figs 2 and 3. Compounds **1** and **2** show a

Table 1. UV–visible absorption and fluorescence emission data for **1**–**3**

Compound	Solvent	$\lambda_{abs\ max}$ (nm)	($\lambda_{f\ max}$) (nm)	$\lambda_{ex\ max}$ (nm)	Stokes shift (cm^{-1})	Φ_f
1	*n*-C_7H_{16}	393	511	402	5876	0.051
	CCl_4	403	543	402	6397	0.311
	Dioxane	404	554	403	6702	0.516
	THF	414	581	407	6943	0.457
	EtOAc	409	583	403	7297	0.089
	CH_3OH	413	567	416	6577	0.003
	DMF	428	638	425	7691	0.040
	CH_3CN	410	642	405	8814	0.009
2	*n*-C_7H_{16}	403	509	398	5167	0.076
	CCl_4	413	531	406	5381	0.521
	Dioxane	416	565	404	6339	0.869
	THF	423	592	421	6749	0.324
	EtOAc	414	592	413	7263	0.090
	CH_3OH	418	558	418	6002	0.003
	DMF	432	642	426	7562	0.093
	CH_3CN	419	650	410	8482	0.001
3	*n*-C_7H_{16}	357	403, 424, 520	356	3198	0.004
	CCl_4	366	407, 428, 522	364	8165	0.007
	Dioxane	369	418, 529	371	8197	0.047
	THF	368	542	372	8723	0.121
	EtOAc	367	547	371	8966	0.095
	CH_3OH	367	417, 546	372	8932	0.002
	DMF	376	585	374	9501	0.149
	CH_3CN	369	593	369	10237	0.066

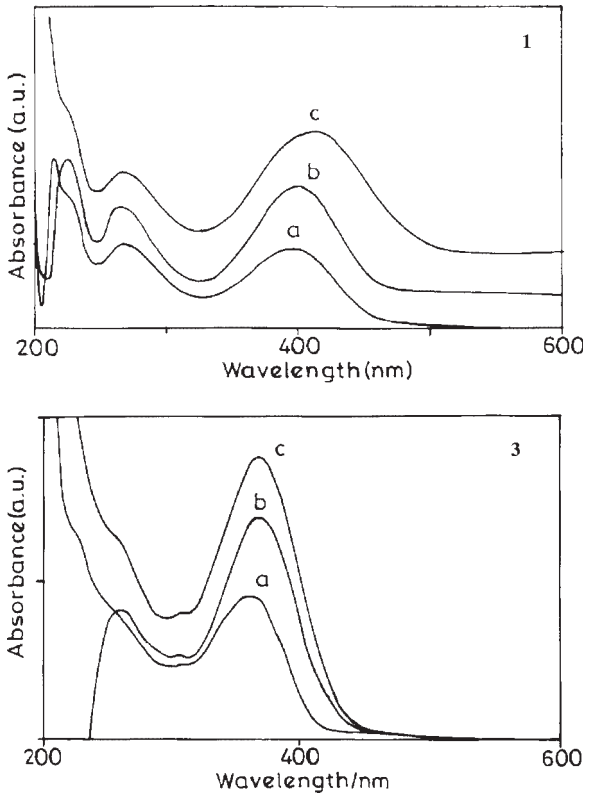

Figure 1. UV–visible absorption spectra of (top) **1** and (bottom) **3** in (a) heptane, (b) 1,4-dioxane and (c) methanol

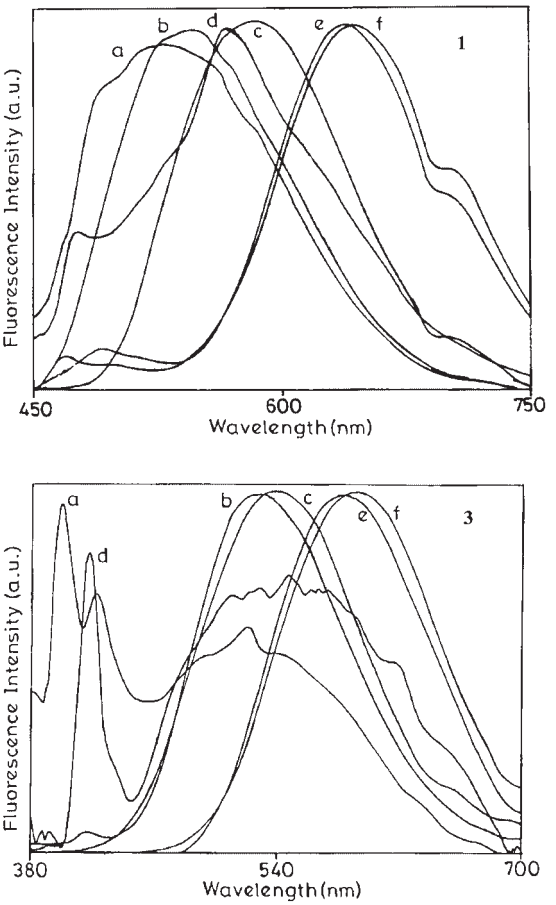

Figure 2. Fluorescence spectra of (top) **1** and (bottom) **3** in (a) heptane, (b) 1,4-dioxane, (c) tetrahydrofuran, (d) methanol, (e) dimethylformamide and (f) acetonitrile

single fluorescence band in all the solvents examined. However, this band is red-shifted with increasing solvent polarity. On the other hand, **3** shows three fluorescence bands located at 403, 424 and 520 nm in the non-polar solvent heptane. In medium-polarity and polar solvents, however, the fluorescence emission bands of **3** at the shorter wavelengths are minimized and the longer wavelength fluorescence emission band at 520 nm is red-shifted. On going from the non-polar solvent heptane to the aprotic polar solvent acetonitrile, the longer wavelength fluorescence emission bands of **1–3** are red-shifted by 131, 141 and 73 nm, respectively. Such large solvatochromic shifts of the fluorescence emission are characteristic of nitro-substituted arylindolic ethenes. It may be noted that the ethenyl compounds bearing a *p*-aminophenyl group, e.g. 3-(4-aminophenylethenyl-*E*)-NH-indole, show only a very moderate solvent polarity effect on their absorption and fluorescence spectra.[26] Hence, the remarkable solvatochromic effect in **1–3** is due to the electron-withdrawing nature of the nitro group. It is therefore suggested that in their excited state the nitro-substituted compounds **1–3** interact strongly with the polar environment.

The excitation spectra of **1** and **3** are shown in Fig. 3. The excitation spectrum is similar to the absorption spectrum of these compounds, which indicates that the fluorescence emissions in these compounds originate from a single ground-state species. The excited-state lifetimes of these compounds are shown in Table 2. The fluorescence decay curves for **1** and **3** in 1,4-dioxane are shown in Fig. 4. The fluorescence decays are multi-exponential in non-polar heptane. However, **1** and **2** show single-exponential decay in medium-polarity and polar solvents. This indicates that more than one type of singlet excited state is involved in the photoprocesses of these compounds. Two of the excited species have shorter life times (0.1–1 ns), whereas the third one has a longer lifetime (1–4 ns). The amplitude data suggest that the shorter lifetime species dominates over the longer lifetime species.

A plot of Stokes shift vs solvent polarity parameters such as Δf[35] and $E_T(30)$[38] are shown in Figs 5 and 6, respectively. The change in excited-state dipole moment ($\Delta\mu$) for **1–3** is calculated to be 15.87, 16.45 and 16.33 D, respectively. Hence, the excited-state dipole moment (μ_e) for **1–3** is 24.37, 25.36 and 24.19 D, respectively. From the plot of Stokes shift vs $E_T(30)$, it is observed that all three ethenes show a large ΔG value with maximum 191.3 kcal mol^{-1} for **1** and minimum 183.8 kcal mol^{-1} for **3** (Table 3) (1 kcal = 4.184 kJ). This means that the singlet excited states of **1–3** are highly polar in nature and, hence, a strong interaction of the excited state of

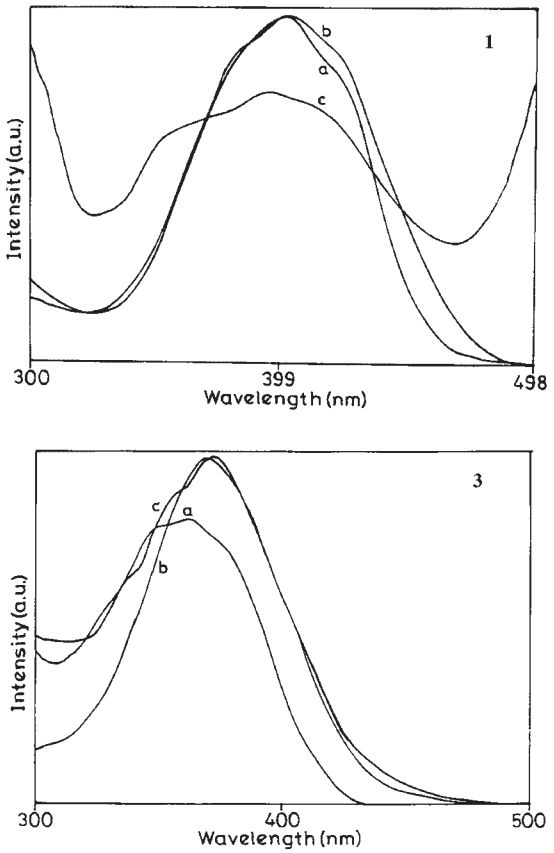

Figure 3. Fluorescence excitation spectra of (top) **1** and (bottom) **3** in (a) heptane, (b) 1,4-dioxane and (c) methanol

these compounds with the solvent molecules is expected. A plot of the Φ_f against solvent polarity parameter $E_T(30)$ is shown in Fig. 7. The Φ_f for **1**–**3** increases with increasing solvent polarity, with a maximum in 1,4-dioxane, (**1**, 0.516; **2**, 0.869; **3**, 0.047). However, Φ_f falls off drastically in polar solvents with a minimum in methanol for **1**–**3** (**1**, 0.003; **2**, 0.003; **3**, 0.002). The Φ_f for **3** is lower than those for **1** and **2**. The existence of large solvatochromic fluorescence and multiple fluorescence decay behaviors indicates the presence of more than one excited state in the photoprocesses of these compounds (Scheme 2). These states can be locally excited state (LE), intramolecular charge-transfer excited state (ICT) and conformationally relaxed intramolecular charge-transfer excited state (CRICT) as found in other donor–acceptor compounds[23–29]. In **1** and **2**, all three species are found in non-polar solvents, whereas in medium-polarity and polar solvents, the CRICT species is predominantly formed. Hence, the structure of the singlet excited state is highly sensitive to specific solute–solvent interactions and the fluorescing species may not be the same in every polar solvent. The extent of conformational relaxation of the locally excited singlet state and the resultant charge transfer depended greatly on the nature of the surrounding media.

Photoisomerization

Direct irradiation of a solution of **1** and **2** in heptane, 1,4-dioxane and methanol does not yield any photoisomerized product, as revealed by the UV–visible absorption and the HPLC analyses. There was no change in the UV–visible spectrum of **1** and **2** even after 8 h of irradiation. The HPLC analysis showed only one peak with $t_R = 8.3$ min (20% ethyl acetate–hexane, 2.0 ml min^{-1}) and $t_R = 6.66$ min (15% ethyl acetate in hexane, 1.1 ml min^{-1}) corresponding to **1** and **2**, respectively. On the other hand, **3**, having an electron-withdrawing phenylsulfonyl substituent at the indolic nitrogen, on irradiation undergoes *trans–cis* photoisomerization as evidenced by the UV–visible absorption and the HPLC analyses of the photomixture. The HPLC analysis of the photomixture of **3** showed the presence of two components, one with $t_R = 13.3$ min corresponding to *trans*-**3** and the other with $t_R = 12.3$ min due to *cis*-**3** (10% ethyl acetate in hexane, flow rate 1.1 ml min^{-1}) (Fig. 8). A high photoisomerization quantum yield ($\Phi_{t\rightarrow c}$, 0.50 in heptane, 0.31 in 1,4-dioxane and 0.21 in methanol) in all the three solvents is observed for **3**. The photostationary state composition is given in Table 4.

The efficiency of *trans–cis* isomerization decreases on increasing the solvent polarity. On absorption of light, these ethenes yield a highly polar excited state. In polar

Table 2. Fluorescence lifetime and amplitude data for **1**–**3**

		Lifetime [τ (ns)]/amplitude (α)							
Compound	Solvent	τ_1	α_1	τ_2	α_2	τ_3	α_3	τ_{av} (ns)	χ^2
1	n-C_7H_{16}	0.036	0.725	0.224	0.255	1.814	0.020	0.120	1.32
	Dioxane	—	—	—	—	2.68	1.0	2.68	1.02
	CH_3OH	—	—	—	—	0.10	1.0	0.10	1.10
2	n-C_7H_{16}	0.016	0.714	0.223	0.254	1.023	0.034	0.104	1.35
	Dioxane	—	—	—	—	2.707	1.0	2.707	1.08
	CH_3OH	—	—	—	—	0.15	1.0	0.15	1.20
3	n-C_7H_{16}	0.045	0.472	0.728	0.359	3.189	0.169	0.847	1.18
	Dioxane	0.138	0.519	0.901	0.445	2.067	0.036	0.547	1.23
	CH_3OH	0.026	0.791	0.594	0.170	4.359	0.039	0.293	1.09

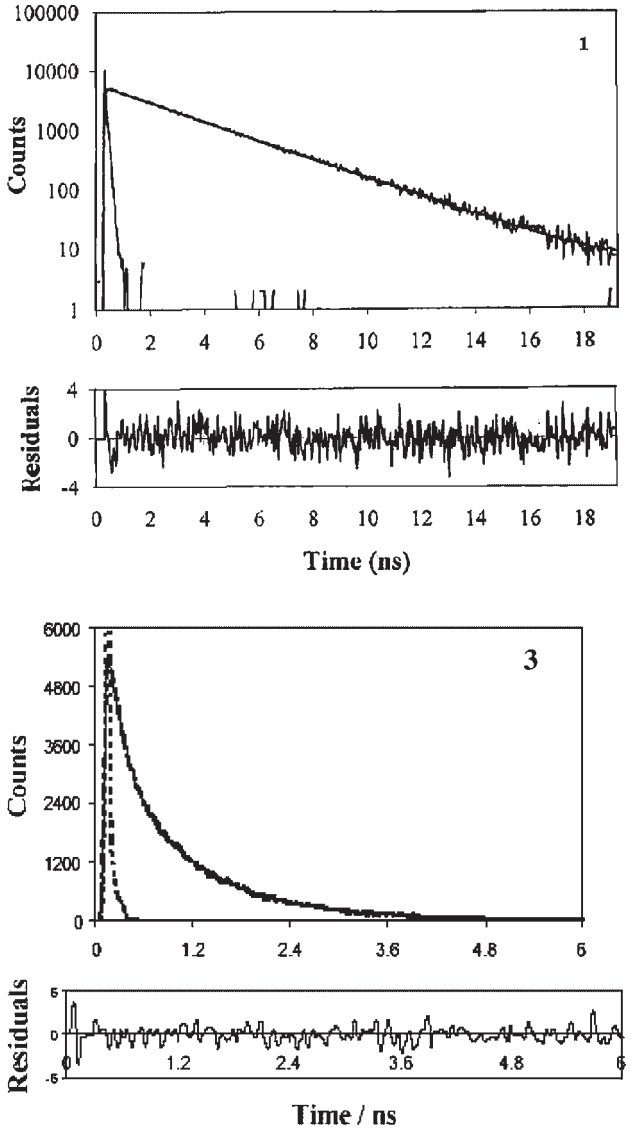

Figure 4. Fluorescence decay profiles for (top) **1** and (bottom) **3** in 1,4-dioxane

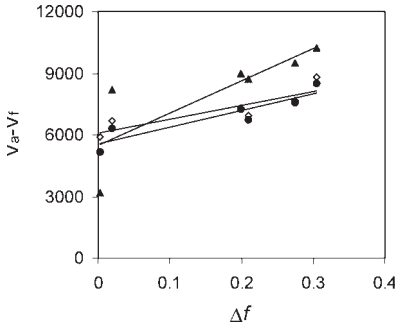

Figure 5. Lippert–Mataga plot: Stokes shift vs solvent polarity parameter (Δf) for (diamonds) **1**, (circles) **2** and (triangles) **3** in organic solvents of varying polarity

solvent, a net stabilization of the excited state can cause a large energy barrier for the photoisomerization process. Hence, the efficiency of *trans–cis* isomerization is lower in polar solvents. The small $\Phi_{t\rightarrow c}$ for **3** in polar solvents

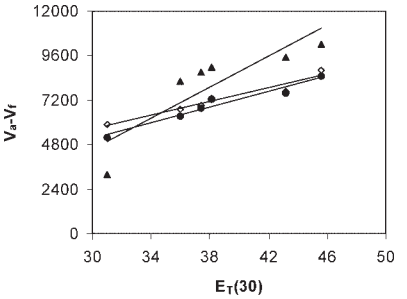

Figure 6. Plot of Stokes shift vs solvent polarity parameter $E_T(30)$ for (diamonds) **1**, (circles) **2** and (triangles) **3** in organic solvents of varying polarity

indicates an efficient deactivation process other than *trans–cis* isomerization for *trans*-**3** from its excited singlet state.

The singlet excited-state energy for these compounds is calculated by taking the intersection wavelength of fluorescence excitation and emission spectra in heptane and methanol and using the approximate equation $S_1 - S_0 = hc/\lambda = 1.24\,\text{keV}/\lambda$, where, h (Planck's constant) $= 6.62 \times 10^{-34}$ J s, c (velocity of light) $= 3 \times 10^8\,\text{m s}^{-1}$ and $\lambda =$ wavelength in nanometers. From heptane to methanol, it is found that the singlet excited-state energy varies from 2.66 to 2.74 eV for **1** and **2**, whereas it is 3.04–3.26 eV for **3**. This indicates that the singlet-state energy of **3** is 0.52 eV higher than those of **1** and **2** (Scheme 3).

The activation energy barrier to the phantom excited state (P*) in *trans*-stilbene is known to be increased in the presence of a donor substituent or donor–acceptor conjugation effect.[39–41] Hence, such compounds follow the radiative pathway rather than the P* pathway. This is also corroborated by their relatively higher Φ_f. Here, we expect that compared with **1** and **2**, **3** has a lower energy barrier to the P* state because of the electron-withdrawing nature of —$SO_2C_6H_5$. Hence, **3** follows both the radiative and the P* pathways, whereas **1** and **2** follow the radiative pathway predominantly.

Again, the trends observed for Φ_f for **1** and **2** and Φ_f and $\Phi_{t\rightarrow c}$ for **3** indicate competitiveness of the observed photoprocesses, i.e. fluorescence emission and photoisomerization. It can be suggested that photoisomerization of **3** occurs from its singlet excited state. Hence **3** is photochemically active, whereas **1** and **2** are photochemically stable (Scheme 4).

Linear free energy relationship

The sensitivity (ρ) towards the formation of CRICT state and photoisomerization process is determined by the Hammett concept of linear free energy relationship (LFER)[42,43] and using the following equation:

$$\log(k/k_0) = \sigma\rho$$

Table 3. Dependence of fluorescence spectral data on solvent polarity parameters

	$E_T(30)$		Δf			μ (D)	
Compound	R^2	Slope	R^2	Slope	$\Delta\mu$ (D)	μ_g (D)	μ_e (D)
1	0.94	191.3	0.94	5914	15.87	8.50	24.37
2	0.95	189.9	0.89	6351	16.45	8.91	25.36
3	0.80	183.8	0.90	6265	16.33	7.86	24.19

R^2, linear correlation; $\Delta\mu$, dipole moment change as obtained by Lippert–Mataga plot by taking Onsager radius 7.3 Å and using dielectric constant (ε) and refractive index (η) of the solvent; parameters are calculated without considering solvent heptane, owing to deviation from the Lippert–Mataga and $E_T(30)$ plots for **3** (Figs 5 and 6); μ_g is the ground-state dipole moment as calculated by the Hyperchem semiempirical AM1 method.

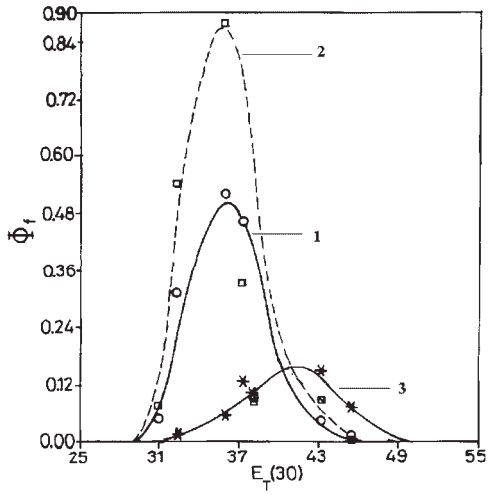

Figure 7. Plot of fluorescence quantum yield (Φ_f) vs $E_T(30)$ value for (circles) **1**, (squares) **2** and (asterisks) **3** in organic solvents of varying polarity

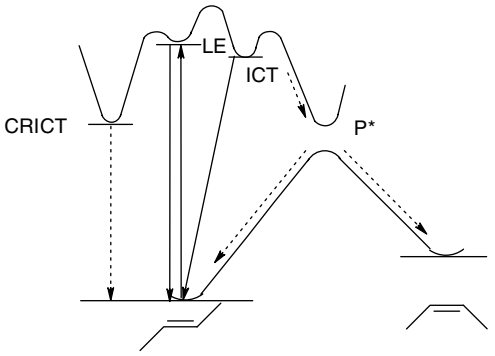

Scheme 2. Three-state kinetic scheme applicable to *p*-nitrophenylindolic ethenes. LE, locally planar excited state; ICT, intramolecular charge-transfer excited state; CRICT, conformationally relaxed intramolecular charge-transfer excited state; P*, perpendicular double bond twisted excited-state species (phantom excited state)

where k is the rate constant when a substituent is present in the molecule, k_0 is the rate constant when the substituent is hydrogen atom, σ is the Hammett substituent constant and ρ is the sensitivity of the reaction.

On excitation to the singlet excited state, the *trans* configuration undergoes a conformational relaxation owing to the solvent–solute interaction, which leads to a more stable CT excited state, from which fluorescence occurs. These relaxation processes result in a Stokes shift (ΔE).

Hence the above Hammett equation can be used as $\Delta E/2.3kT = \sigma\rho$, where, k is the Boltzmann constant (1.38×10^{-23}); T is the absolute temperature, σ is the relative value between the nitro and the substituent present on the indolic nitrogen ($\sigma_{NO_2} - \sigma_R$). Sensitivity (ρ) of photoprocesses in various solvent with increasing solvent polarity is calculated from the slope of the plot,

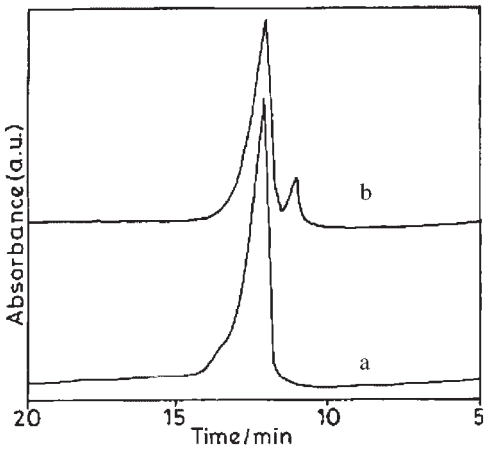

Figure 8. HPLC traces: (a) before and (b) after the irradiation of **3** in 1,4-dioxane

Table 4. Photostationary state (PSS) composition and photoisomerization quantum yield ($\Phi_{t\rightarrow c}$) of **1**–**3**

		PSS composition (%)		
Compound	Solvent	*E*	*Z*	($\Phi_{t\rightarrow c}$)
1	*n*-C_7H_{16}	—	—	—
	Dioxane			
	CH_3OH			
2	*n*-C_7H_{16}	—	—	—
	Dioxane			
	CH_3OH			
3	*n*-C_7H_{16}	48.28	51.72	0.50
	Dioxane	93.42	6.58	0.31
	CH_3OH	94.83	5.17	0.21

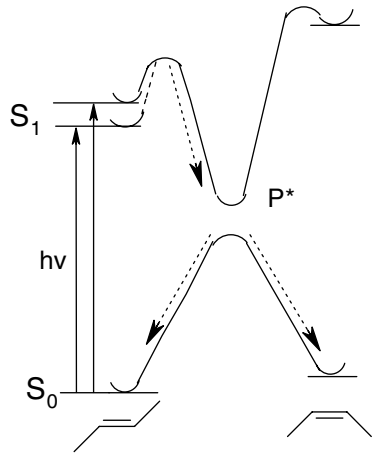

Scheme 3. Plausible energy profiles which show the decrease in the energy barrier between S_1 and P* states in **3**. Dashed line, energy profile in the absence of substituent; solid line, energy profile in the presence of an electron-withdrawing substituent, $SO_2C_6H_5$

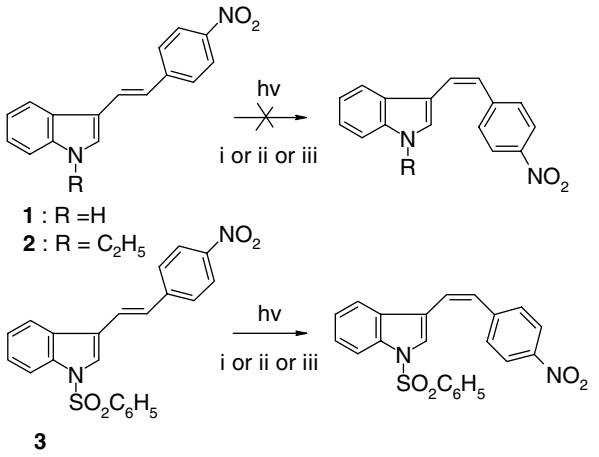

Scheme 4. Photochemical changes of **1**–**3** in (i) heptane, (ii) 1,4-dioxane and (iii) methanol

drawn between ($\Delta E/2.3kT$) vs relative σ-values of the substituent ($\sigma_{NO_2} - \sigma_R$) (Table 5 and Fig. 9) with the assumption that all the molecules lying on the same Hammett plot belong to the same type of charge-transfer species. It is found that on increasing the solvent polarity, the value of $\Delta E/2.3kT$ increases, which indicates strong interaction of the excited state of these molecules with polar solvents. All points on the Hammett plot lie on the straight line, except for **3** in the non-polar solvents *n*-heptane and CCl_4, when we consider the shorter wavelength emission maximum for calculation of the Stokes'shift/$2.3kT$ parameter. This deviation for **3** is because of the presence of a species different from the CRICT species in heptane and CCl_4. The ρ value is negative, which indicates the formation of an electron-deficient cationic excited-state species. Hence the excited state is stabilized more in the presence of an electron donor substituent, such as ethyl, but destabilized in the presence

Table 5. Sensitivity (ρ) of the CRICT state for **1**–**3** in solvents of increasing solvent polarity

Solvent	ρ	R^2	No. of points
n-C_7H_{16}	4.29	0.99	3
CCl_4	3.08	0.95	3
Dioxane	2.24	0.99	4
THF	2.41	0.99	4
EtOAc	2.19	0.98	4
DMF	2.55	0.97	4
CH_3CN	2.18	0.98	4

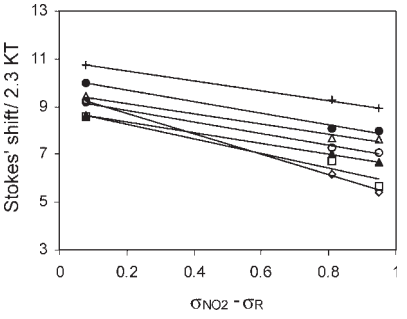

Figure 9. Plot of Stokes shift/$2.3kT$ vs relative Hammett σ constant ($\sigma_{NO_2} - \sigma_R$): (diamonds) heptane, (squares) CCl_4, (closed triangles) 1,4-dioxane, (open circles) THF, (open triangles) ethyl acetate, (closed circles) DMF and (plus) acetonitrile

of an electron-withdrawing substituent, such as benzenesulfonyl. Similarly, the cationic excited state is stabilized more in the presence of polar solvents rather than the non-polar solvents *n*-heptane and CCl_4. Therefore, a high ρ value is observed in non-polar solvents, whereas in medium-polarity and polar solvents a comparable ρ value is observed. In other words, the cationic excited state is less stabilized in the presence of an electron-withdrawing substituent and in an non-polar solvent. Therefore, the excited state is close to the P* state, which leads to efficient photoisomerization in the case of **3**.

CONCLUSION

Absorption and fluorescence studies together with correlation of these spectroscopic properties with various solvent polarity parameters reveal the highly polar nature of the singlet excited state of push–pull ethenylindoles. Time-resolved fluorescence studies together with Lippert–Mataga, $E_T(30)$ and LFER plots show that these compounds contain three type of excited species, namely LE, ICT and CRICT, the formation of which depended greatly on the solvent polarity and the substituent present on the indolic nitrogen atom. The LFER plots indicate a cationic excited state, which is stabilized more in the presence of an electron-releasing substituent such as

ethyl and in medium-polarity and polar organic solvents. Compounds **1** and **2** are photochemically stable, whereas **3** is photoactive and undergoes efficient photoisomerization in the non-polar solvent heptane. Further, the trend of Φ_f and $\Phi_{t\rightarrow c}$ in **3** is inversely related. This indicates that the photoisomerization in **3** occurs from the singlet excited state. The energy barrier to photoisomerization is controlled by the substituents and solvents. Thus, ethenylindoles exhibit fluorescence due to CT states and it is possible to alter the absorption, fluorescence and photoisomerization properties of these compounds by changing the donor ability of the indole moiety. Such push–pull systems can be useful for developing materials having newer opto-electronic properties.

Acknowledgments

A research fellowship to P.K.H. from the University Grants Commission, New Delhi, is gratefully acknowledged. Thanks are also due to Professor N. Periasamy for his help in time-resolved fluorescence studies.

REFERENCES

1. Zeichmeister L. *Cis–trans Isomeric Carotenoids—Vitamin A and Aryl Polyenes*. Academic Press: New York, 1962; 158–188.
2. Saltiel J, Zafiriou OC, Megarity ED. *J. Am. Chem. Soc*. 1968; **90**: 4759–4760.
3. Allen MT, Whitten D. *Chem. Rev.* 1989; **89**: 1691–1702.
4. Waldeck DH. *Chem. Rev.* 1991; **91**: 415–436.
5. Gorner H, Kuhn HJ. *Adv. Photochem*. 1995; **19**: 58–115.
6. Arai T, Tokumaru K. *Adv. Photochem*. 1995; **20**: 1–57.
7. Salem L. *Acc. Chem. Res*. 1979; **12**: 87–92.
8. Findlay JBC, Pappin DJC. *Biochem. J*. 1986; **238**: 625–642.
9. Birge RR. *Biochim. Biophys. Acta* 1990; **1016**: 293–327.
10. Gartner W, Towner P. *Photochem. Photobiol*. 1995; **62**: 1–16.
11. Pepe IM. *J. Photochem. Photobiol. A: Biol*. 1999; **48**: 1–10.
12. Dugave C, Demange L. *Chem. Rev.* 2003; **103**: 2475–2532.
13. Meir H. *Angew. Chem. Int. Ed. Engl*. 1992; **31**: 1399–1420.
14. Verbiest T, Burland DM, Jurich MC, Lee VY, Miller RD, Volksen W. *Science* 1995; **268**: 1604–1606.
15. Lambert C, Stadler S, Bourhill G, Brauchle C. *Angew. Chem. Int. Ed. Engl*. 1996; **35**: 644–646.
16. Muthuraman M, Masse R, Nicoud JF, Desiraju GR. *Chem. Mater.* 2001; **13**: 1473–1479.
17. Johnson ID, Thomas EW, Cundall RB. *J. Chem. Soc., Faraday Trans 2* 1985; **81**: 1303–1315.
18. Lin CT, Guan HW, McCoy RK, Spangler CW. *J. Phys. Chem*. 1989; **93**: 39–43.
19. Gruen H, Gorner H. *J. Phys. Chem.* 1989; **93**: 7144–7152.
20. Sonoda Y, Kwok WM, Petrasek Z, Ostler R, Matousek P, Parker AW, Phillips D. *J. Chem. Soc., Perkin Trans. 2* 2001; 308–314.
21. Singh AK, Mahalaxmi GR. *Proc. Natl. Acad. Sci., Sect. A: Phys. Sci. (India)* 2000; **70**: 1–26.
22. Lapouyade R, Kuhn A, Letard JF, Rettig W. *Chem. Phys. Lett*. 1993; **208**: 48–58.
23. Singh AK, Mahalaxmi GR. *Photochem. Photobiol*. 2000; **71**: 387–396.
24. Singh AK, Darshi M, Kanvah S. *J. Phys. Chem. A* 2000; **104**: 464–471.
25. Singh AK, Kanvah S. *J. Chem. Soc., Perkin Trans. 2* 2001; 395–401.
26. Singh AK, Hota PK. *Indian J. Chem.* 2003; **42B**: 2048–2053.
27. Pines D, Pines E, Rettig W. *J. Phys. Chem. A* 2003; **107**: 236–242.
28. Yang JS, Liau KL, Wang CM, Hwang CY. *J. Am. Chem. Soc.* 2004; **126**: 12325–12335.
29. Iyichev YV, Kuhnle W, Zachariasse KA. *J. Phys. Chem. A* 1998; **102**: 5670–5680.
30. Zachariasse KA. *Chem. Phys. Lett.* 2000; **320**: 8–13.
31. Sobolewski AL, Domcke W. *Chem. Phys. Lett.* 1996; **250**: 428–436.
32. Sobolewski AL, Sudholt A, Domcke W. *J. Phys. Chem. A* 1998; **102**: 2716–2722.
33. Rabek JF. *Experimental Methods in Photochemistry and Photophysics, Part 2*. Wiley: Chichester, 1982; 746–790.
34. Dewar MJS, Zoebisch EG, Healy EF, Stewart JJP. *J. Am. Chem. Soc*.1985; **107**: 3902–3909.
35. Lippert E, Luder W, Moll F, Nagele H, Boos H, Prigge H, Blankenstein IS. *Angew. Chem.* 1961; **73**: 695–706.
36. Lide DR (ed). *CRC Handbook of Chemistry and Physics* (79th edn). CRC Press: Boca Raton, FL, 1998–1999; Section 8–120.
37. Rabek JF. *Experimental Methods in Photochemistry and Photophysics, Part 2*. Wiley: Chichester, 1982; 944–946.
38. Reichardt C. *Solvents and Solvent Effects in Organic Chemistry*. Verlag Chemie: Weinheim, 1990; 285–338.
39. Saltiel J, Waller AS, Sears DF Jr, Hoburg EA, Zeglinski DM, Waldeck DH. *J. Phys. Chem.* 1994; **98**: 10689.
40. Papper V, Pines D, Likhtenshtein G, Pines E. *J. Photochem. Photobiol. A: Chem.* 1997; **111**: 87–96.
41. Yang JS, Chiou SY, Liau KL. *J. Am. Chem. Soc.* 2002; **124**: 2518–2527.
42. March J. *Advanced Organic Chemistry, Reactions, Mechanism and Structure* (4th edn). Wiley: New York, 1999; 273–286.
43. Papper V, Likhtenshtein GI. *J. Photochem. Photobiol. A: Chem*. 2001; **140**: 39–52.